CHAPTER III

CHAPTER III

STRUCTURAL, MICROSCOPIC, OPTICAL AND TRANSPORT PROPERTIES OF SnS THIN FILMS

3.1	Introduction	39
3.2	Experimental Details	39
3.2.1	Thickness measurement	39
3.2.2	X-Ray diffraction	40
3.2.3	Scanning electron microscopy (SEM)	40
3.2.4	Optical absorption measurements	40
3.2.5	Measurements on the transport properties	41
	a) Electrical conductivity measurements	41
	b) Thermoelectric power measurements	43
3.3	Discussion of Results	45
3.3.1	X-Ray diffraction studies	45
3.3.2	SEM studies	47
3.3.3	Optical studies	47
3.3.4	Electrical transport studies	49
	a) Conductivity studies	49
	b) Thermoelectric power studies	53
3.4	Conclusions	60
	References	62

3.1 Introduction

The method of materials formation and its composition are responsible for its properties /1,2/. Therefore growth along a particular direction and under controlled conditions is essential. Chapter II highlights few of the preparation parameters and deposition conditions necessary to achieve good quality deposition of SnS thin films. As our intention is to use these SnS films for photoelectrochemical applications, it is worth to understand the materials aspects such as structure, surface morphology, composition, spectral selectivity, type of conduction, defect states etc. Therefore in these investigations we have prepared SnS thin films by a solution growth process in a very simple and extremely convenient way and with the least consumption of the basic materials /3-5/ and characterized them through the structural, microscopic, optical and the electrical transport properties to obtain the valuable informations on the materials aspects of the SnS.

This chapter is therefore devoted to the necessary designs/ fabrications and experimental techniques that were used in preparing and characterizing the SnS thin films through the above properties.The SnS samples used in these studies were obtained onto the glass substrates as discussed earlier/3,5/ (chapter II, section 2.2.3). The different techniques and several processing steps to characterize these samples are as under.

3.2 Experimental Details

3.2.1 Thickness measurement

The film layer thickness was measured by a weight differnce-density method. The layer thickness (t), mass (m), density (d) and area (A) are related as

$$t = m / A .d \quad \ldots (3.1)$$

where, m = mass of the sample in gram,

a = area of the sample in cm^2, and

d = density of the material in gm/ cm^3 (for SnS d = 5.08 gm/ cm^3).

3.2.2 X-Ray diffraction (XRD)

The structure and crystallinity of the samples both as-deposited and baked(at 100 ^{0}C) were examined by an X-ray diffraction technique. A Philips – PW 1710 X-ray diffractometer (with CuK_α line, λ= 1.5406 A^o) was used for this purpose. The range of 2θ angles was from 10^0 to 80^o . The X-ray diffractograms were further analyzed to determine the crystal structure, lattice dimensions, crystal orientation, crystallite size etc.

3.2.3 Scanning electron microscopy (SEM)

The surface morphology of the samples (as-deposited and baked) was observed through a scanning electron microscope, Stereoscan- 250, MK (III), Cambridge Instrument Ltd. , U.K. Coating used was gold, 1 μm thick.

3.2.4 Optical absorption measurements

The estimation of the optical energy gap and absorption coefficient were done from these measurements. The type of optical transitions was also determined. Actually measurements were performed to determine the optical density as a function of the wavelength. A double beam spectrophotometer, Hitachi- 330 (Japan), was used for this purpose. The range of wavelengths used was from 350 nm to 1000 nm.

3.2.5 Measurements on the transport properties

a) Electrical conductivity measurements

The dc electrical conductivity of the sample, in dark, was measured using a two point probe conductivity measuring unit designed and fabricated in our laboratory. The unit is shown in figure 3.1 and it consists of two brass plates of the dimension 10 cm x 5 cm x 0.6 cm fitted one over the other. The lower plate is fitted tightly on an asbestos base of the dimension 10 inch x 10 inch. Two strip heaters (65W) were kept in parallel on the lower brass plate and other plate was fixed tightly to the lower plate so as to make a sandwich of the heaters between the two plates. A thick multilayered mica sheet was used to wrap the heaters before being put in between the brass plates so as to achieve the electrical insulation. An aluminium sample holder of the dimension 3cm x 0.5 cm x 0.6 cm was designed, fabricated and fixed exactly at the centre of the upper plate. A sample whose conductivity was to be measured was mounted with a copper point press contacts below the sample holder. The area under consideration was defined with rest of the sample erased. The sample was electrically insulated from the upper brass plate and the sample holder by interposing the mica pieces at the appropriate places. Thermal radiation losses were reduced by covering the whole set up in a bakelite box. The box was coated from inside by means of an asbestos sheet. The working temperature was recorded with a chromel- alumel thermocouple (24 gauge) fitted at the centre on the top of the upper brass plate. A regulated power supply unit was used to pass the current through the sample. A fixed potential drop was applied across the sample and the current was noted for various working temperatures. The current

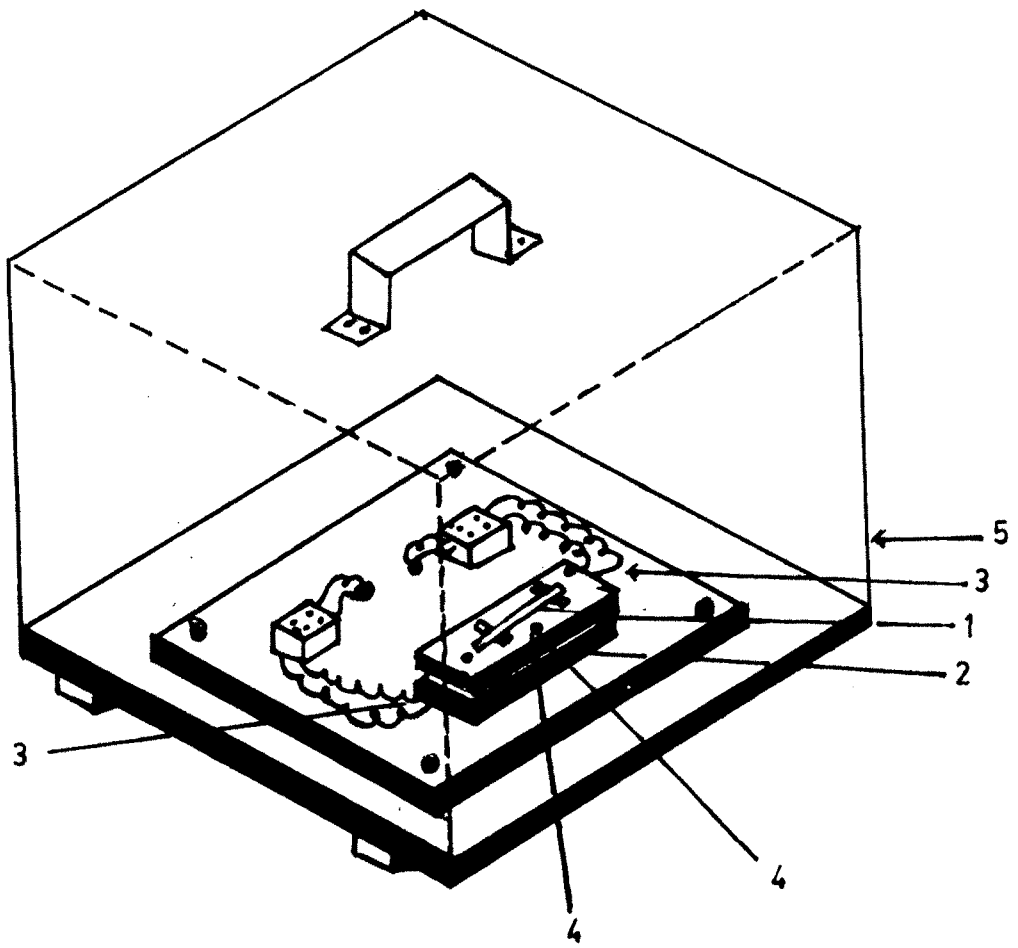

Fig. 3.1 Design and experimental arrangement for the measurement of the electrical conductivity in dark:

1. Sample,
2. Brass plate,
3. Electrical heaters,
4. Thermocouple and
5. Shield.

through the sample was measured using a FET input 4 ½ digit nanoameter, DNM- 121 (Scientific Equipments, Roorkee). The potential drop across the sample was measured with a HIL – 2665 , 4 ½ digit multimeter.

b) Thermoelectric power measurements

Bauerie et al / 6 / have pointed out the know-how's for the measurement of the thermoelectric power. The maximum temperature difference and minimum contact resistance are the major requirements. The thermoelectric power unit was fabricated considering the above requirements. Figure 3.2 shows a schematic of the thermoelectric power measurement unit consisting of the two brass plates of the dimensions 5 cm x 4 cm x 1.2 cm fitted on an asbestos sheet supported by a bakelite sheet. The plates were arranged in parallel separated by a distance of 3cm. They were pitched from the bottom to a size of the miniheaters and the miniheaters of the different wattage (65 W & 35 W) were fixed in them. The electrical insulation between the miniheaters and the brass plates was made. A pair of sample holder, fabricated in a similar fashion as that of the conductivity measurement unit, was fitted on the top adjacent near edges of the brass blocks lengthwise. The sample size used in this measurement was 3.5 cm x 0.5 cm on amorphous glass substrate. The dimension of the substrate holder was 3 cm x 0.5 cm x 0.6 cm. The sample was also electrically insulated from the brass blocks and the substrate holder by means of the mica pieces. The copper press point contacts were used for the measurement. The chromel-alumel thermocouple (24guage) was fixed on the top of the brass blocks for the temperature measurement. The unit was properly shielded by a bakelite box to minimize looses due to

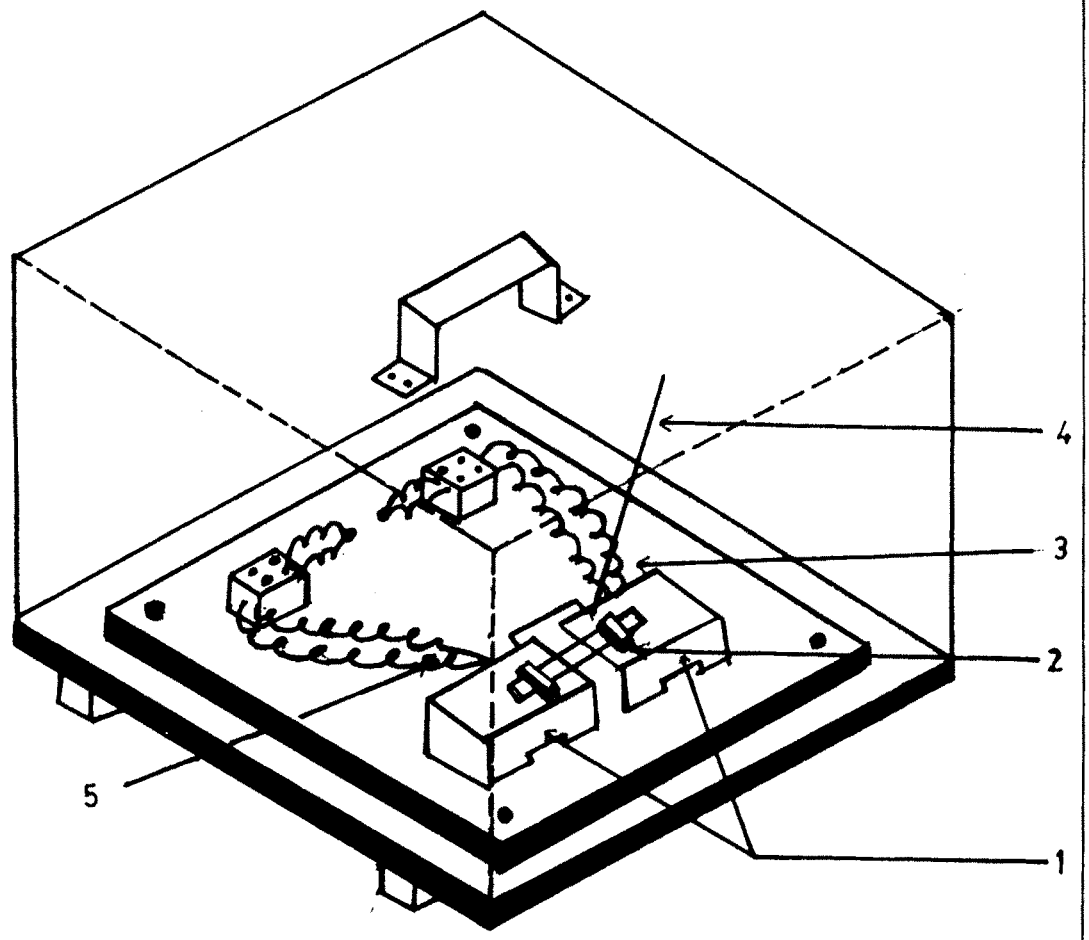

Fig. 3.2 Design and experimental arrangement for the measurements of TEP in dark.

1. Copper blocks,
2. Sample,
3. Thermocouple (mean temperature recorder),
4. Differential thermocouple (thermo-voltage recorder) and
5. Heaters.

the thermal radiations. The thermo voltage generated by a sample was measured using Hewlett Packard, 6 ½ digit multi meter. The temperature gradient was measured with an HIL- 2665, 4 ½ digit microvoltmeter.

3.3 Discussion of Results

3.3.1 X-ray diffraction studies

The X-ray diffraction studies were conducted on the as-deposited and baked SnS samples in the 2θ range of angles between 10^{o} to 80^{o}. The diffractograms were analysed to obtain the informations about the crystallographic aspects. Fig 3.3 shows X-ray diffractograms of a SnS sample before and after baking at 100°C.The analysis of the diffractograms showed that SnS layer has microcrystalline nature with a preferred orientation along (013, 004) direction /3,5/ (table 3.1). The crystal structure is of the orthorhombic type |10| and the calculated lattice parameters are a = 4.02 A^{o}, b = 4.30 A^{o} and c = 11.34 A^{o} /3,5/. These parameters match well with the JCPD data / 7 / and that of the results reported by others /8,9/. The average crystallite size of the microcrystals was determined from the X-ray diffraction patterns. Small crystallites allow the X-ray beam to diverge as it leaves since the diffraction planes are no longer infinite in length as compared to the incident wavelength. Thus these crystallites do not collimate the X-ray beam as effectively as the large crystallites and hence produce a broad diffraction peak /10 /. The average grain size (D) was then determined using a well known Scherrer's relation /10,11/ :

$$D = K\lambda \mid B \cos\theta \qquad \ldots(3.2)$$

where, B is the broadening of the diffraction line measured at half its maximum intensity, λ is the incident wavelength, θ is the diffraction

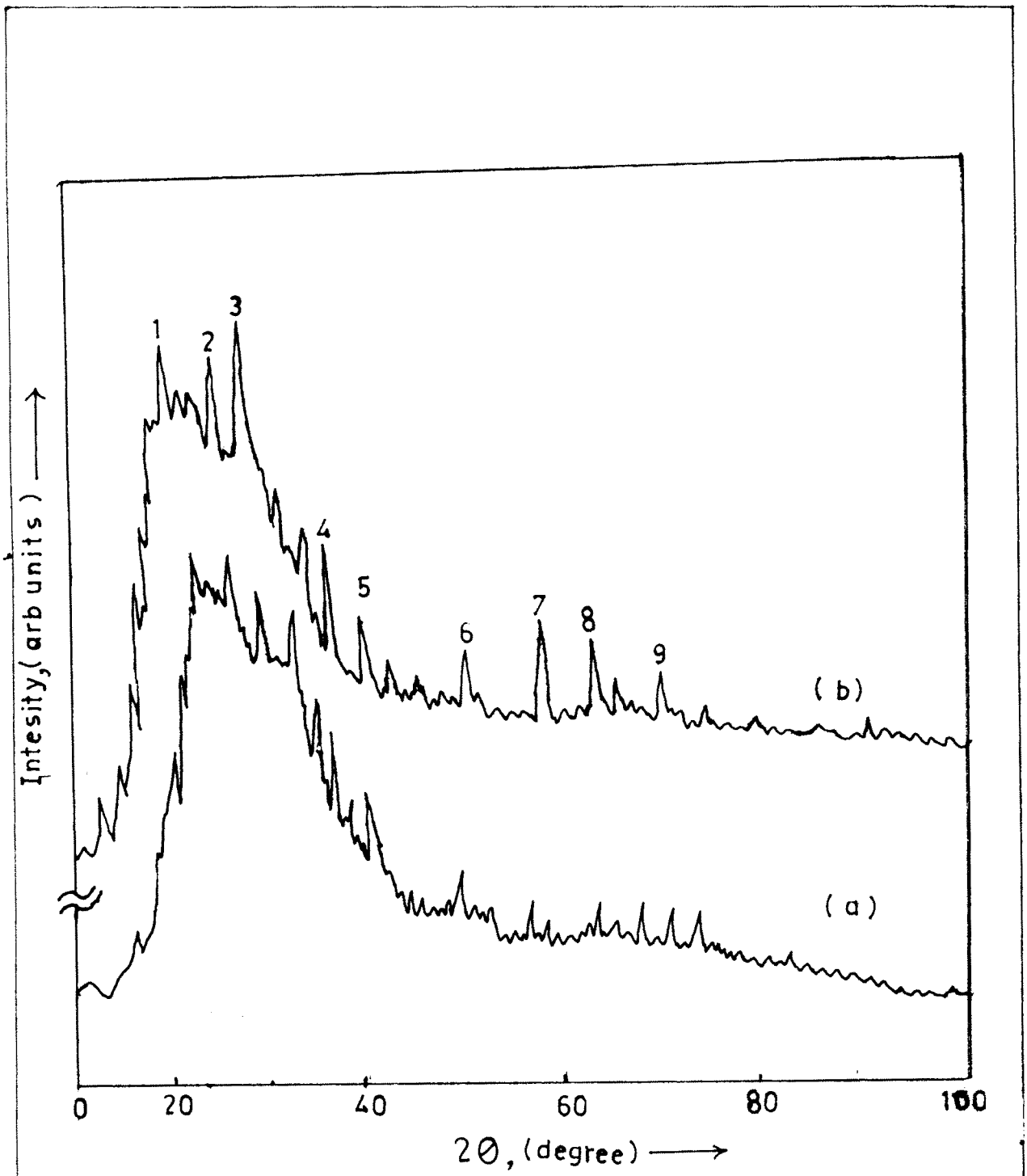

Fig. 3.3 X-ray diffractogram traces of SnS samples.
(a) Unbaked and
(b) Baked (at 100 °C).

angle and K is a constant related to the shape of the crystallites, indices of the reflecting planes etc. The value K = 0.94 represents the best approximation when little is known about the crystallite size and shape. In our case it is seen that the average grain size is 267 A^{o} . Baking of the sample increases the crystalline nature and the crystal size also. The observed crystal size after baking is 376 A^{o}.

3.3.2 Scanning electron microscopy (SEM)

The surface morphology of the SnS thin films (as-deposited and heat treated) was examined through a scanning electron microscope. Fig. 3.4 shows SEM micrographs of a typical sample before and after the heat treatment at 100^{o} C. The as-deposited sample shows very tiny micro crystallites may be randomly oriented and densely packed. After baking at 100^{o} C the SnS sample becomes perfectly crystalline with the presence of spherical well defined grains ($\approx$ 5000 A^{o}) grown at the expense of tiny microcrystallites due to the heat treatment / 3,5,8 /.

3.3.3 Optical Studies

The literature survey points out that the conventional solution growth technique is being widely employed for growth of the binary and ternary compound thin films. If the experimental results on the optical studies are to interpret properly, it is important to know the type of transitions that are taking place in the material under investigation. It is also possible to differentiate direct and indirect type of transitions by examining the energy ($h\nu$) dependence of the absorption coefficient (α) . Therefore, a good quality SnS thin film was further characterized by means of an optical technique. The optical absorption spectrum for SnS thin films was therefore obtained at 300 K in the 350 nm - 1000 nm wavelength range and the absorption coefficient was calculated for

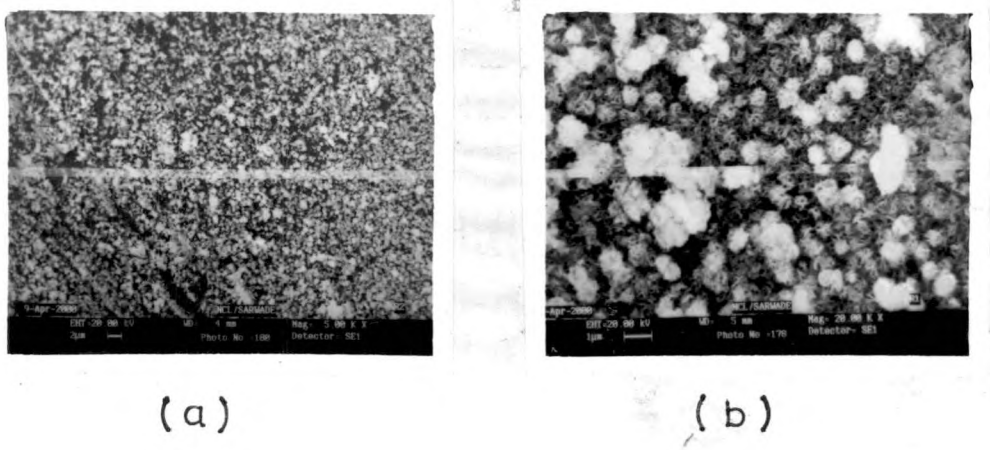

(a) (b)

Fig. 3.4 Microscopic observations of SnS films;

(a) Unbaked and

(b) Baked (at 100 ^{o}C).

each wavelength. The absorption coefficient is high and is of the order of $10^4 - 10^5$ cm $^{-1}$. An energy absorption spectrum is shown in figure 3.5. The spectrum clearly showed that the absorption edge is at around 930 nm. In general, the absorption coefficient (α) and photon energy ($h\nu$) are related as /11-13 / :

$$\alpha = (A / h\nu)\ (h\nu - Eg)^{m} \qquad \ldots (3.3)$$

where, A is a constant and m assumes values ½ , 2, 3/2 and 3 for allowed direct, allowed indirect, forbidden direct and forbidden indirect transitions, respectively. For allowed direct transitions,

$$\alpha h\nu = A\ (h\nu - Eg)^{1/2} \qquad \ldots (3.4)$$

Thus, a plot of $(\alpha h\nu)^2$ vs $h\nu$ should be a straight line whose intercept on the energy axis gives the energy gap, Eg. In our case (fig. 3.6) it is equal to 1.32 eV for untreated sample. This is in close agreement with the previous reports / 3,5,8 /. As suggested by the value of the absorption coefficient and straight line nature of the $(\alpha h\nu)^2$ vs $h\nu$ plot in the high energy region, the mode of optical transitions in this sample is of the band to band direct type. Further equation (3.4) can be rearranged as,

$$\ln(\alpha h\nu) = \ln(A) + 0.5 \ln(h\nu - Eg) \qquad \ldots (3.5)$$

and suggests that the plot of $\ln(\alpha h\nu)$ vs $\ln(h\nu - Eg)$ should be a straight line whose slope must be 0.5 indicating direct type of transitions / 3,5,8 /. Fig. 3.7 was therefore constructed and it is found that the value of m is equal to the 0.5.

3.3.4 Electrical transport studies

a) Conductivity studies

The electrical conductivity of a good sample was measured in dark in the temperature range from 300 K to 550 K. The electrical resistivity decreased with the increase in temperature. Thus SnS exhibits a

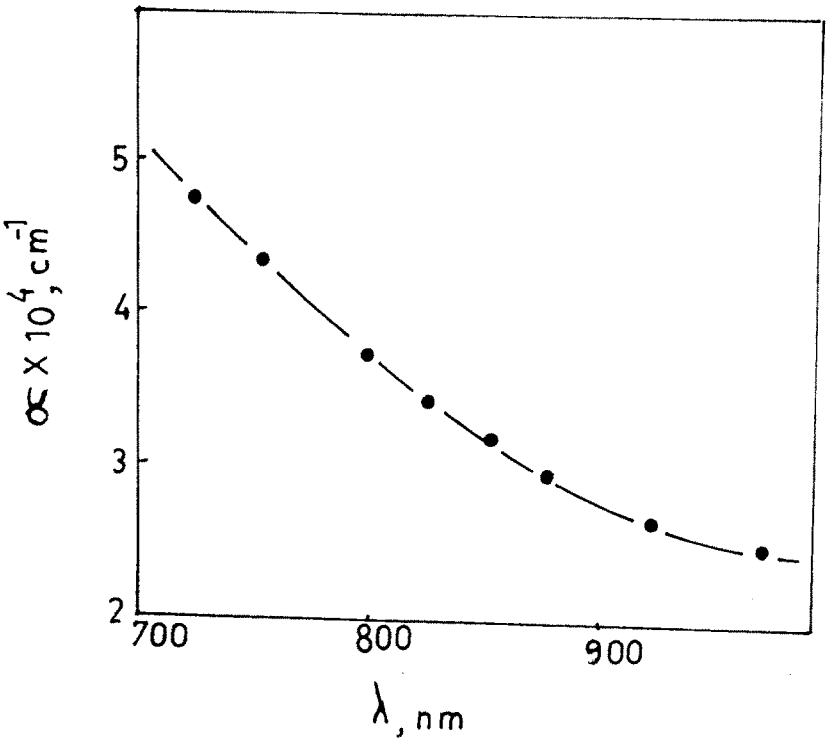

Fig. 3.5 The optical absorption spectra for a SnS film (corrected for glass substrate absorption).

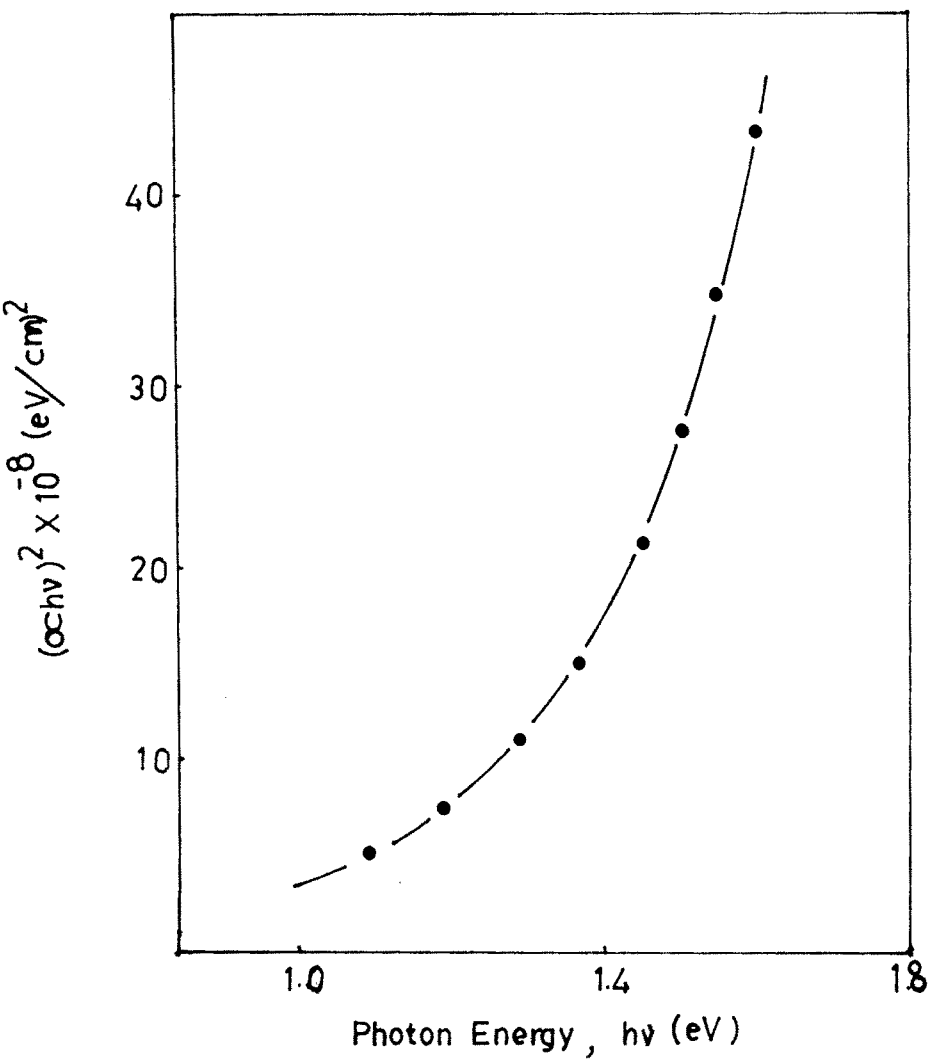

Fig. 3.6 Determination of an optical gap of a SnS film.

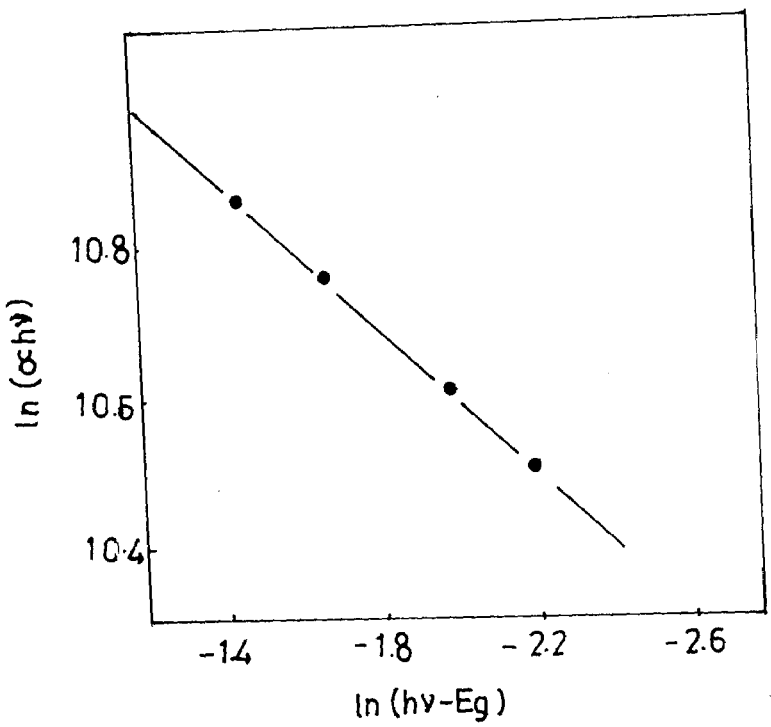

Fig. 3.7 Evaluation of the mode of optical transitions from variation of ln ($\alpha h\nu$) vs ln ($h\nu$-E_g) for the SnS sample.

semiconducting nature. At room temperature, SnS has a typical value of electrical conductivity equal to 10^{-6} $(ohm\text{-}cm)^{-1}$. The temperature variation of logarithmic conductivity is shown in fig. 3.8.

From the plot it is seen that there are two distinct regions. The transition from a straight line region with a low gradient to one with a higher gradient as temperature is increased suggests that more than one conduction mechanisms are involved. For higher temperature region the data could be fitted to an exponential temperature variation of the conductivity,

$$\sigma_{(T)} = \sigma_{(o)} \exp\ (-E_{a\sigma} / kT) \qquad \ldots(3.6)$$

where, $E_{a\sigma}$ is the conductivity activation energy and k is the Boltzman constant. This has indicated the possibility of grain boundary scattering limited conduction mechanism. The conductivity activation energies calculated from the slopes of the linear regions of log σ vs 1/T are 0.12 eV and 0.701 eV in the low and high temperature regions, respectively.

b) Thermoelectric power studies

Another method to characterize the semiconducting materials is the thermoelectric power measurement. This involves measurement of thermally generated voltage of a sample. The technique also helps to detect the type of conductivity of the material under investigation. The thermoelectric power (P) generated by a SnS sample was measured in the temperature range from 300 K to 450 K and the sample is found to be of the p-type conduction. The order of generated thermovoltage is μV. The temperature dependence of thermopower is shown in fig. 3.9.

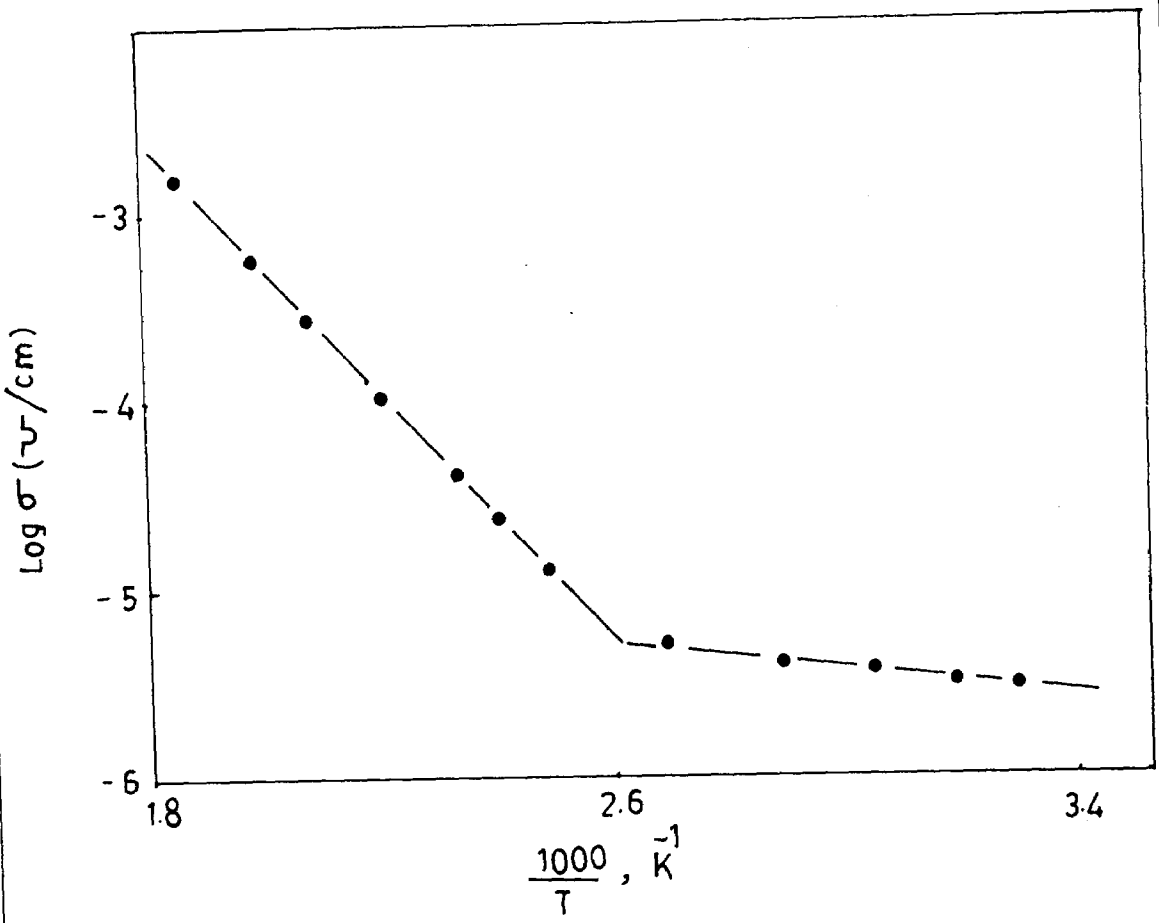

Fig. 3.8 Temperature dependence of an electrical conductivity for a SnS sample.

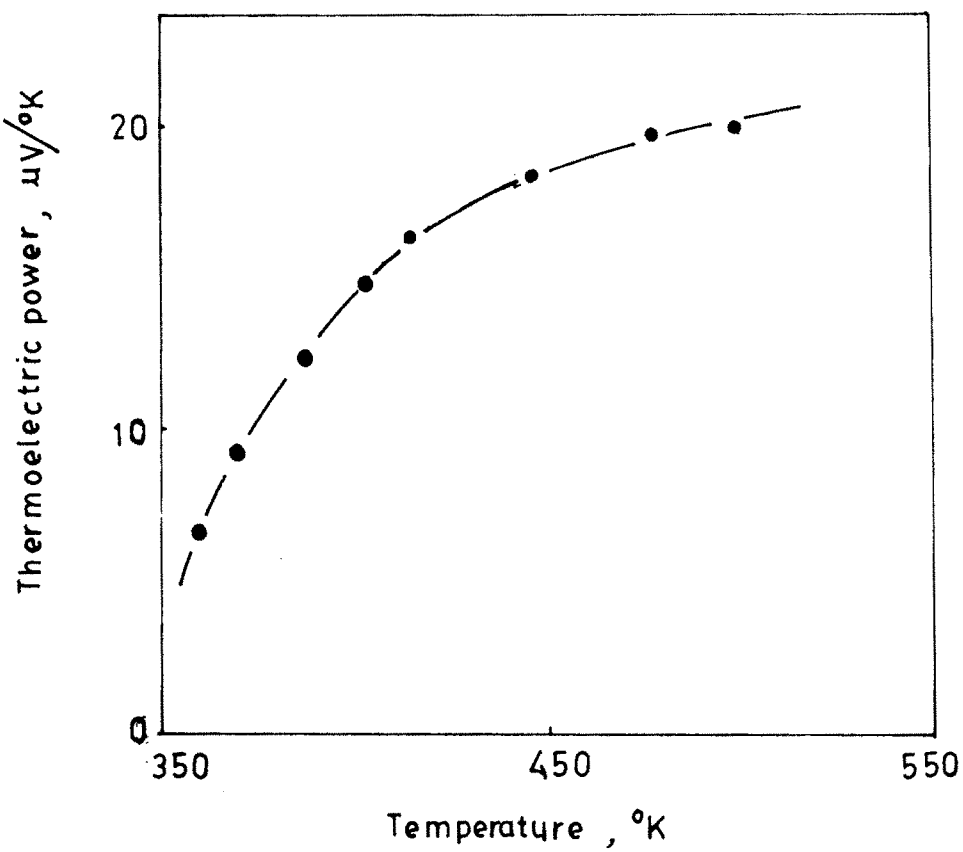

Fig. 3.9 The temperature dependence of thermoelectric power for a SnS sample.

The thermoelectric power (P) varies with the temperature according to the relation / 11,13, 14, 15 / .

$$P = (-k / e) [A + \ln\{2 (2\pi m_h * kT)^{3/2} / ph^3] \quad \ldots (3.7)$$

where, e is an electronic charge, h is the Planck's constant, A is a thermoelectric factor introduced by the kinetic energy of electrons and hence depends on the scattering process, p is the carrier concentration, m_h* is the effective mass of the hole, T is the absolute temperature and k is the Boltzman constant . The thermoelectric power is observed to increase with increase in temperature. The conductivity and thermoelectric power data were utilized to calculate the carrier density. The room temperature magnitude of carrier concentration is 10^{19} cm^{-3}. The temperature dependence of carrier concentration is shown in figure 3.10. The carrier mobilities at different temperatures are determined by using a standard relation

$$\mu = \sigma / p e \ . \quad \ldots(3.8)$$

The dependence of carrier mobility on temperature suggests the possibility of scattering mechanism associated with the inter grain barrier. The temperature dependent grain boundary mobility is related to the grain boundary potential as / 14,16 /;

$$\mu = \mu_o \exp (-\phi_B / kT) \quad \ldots(3.9)$$

where , ϕ_B is the height of the potential barrier at the grain boundary, μ_o is the pre-exponential factor which on the assumption that the current over the barrier flows by thermionic emission, depends on the grain size (d) and the effective carrier mass (m_h*) as / 15,16/ :

$$\mu_o = (qd / 2\pi m_h * k T)^{1/2}. \quad \ldots (3.10)$$

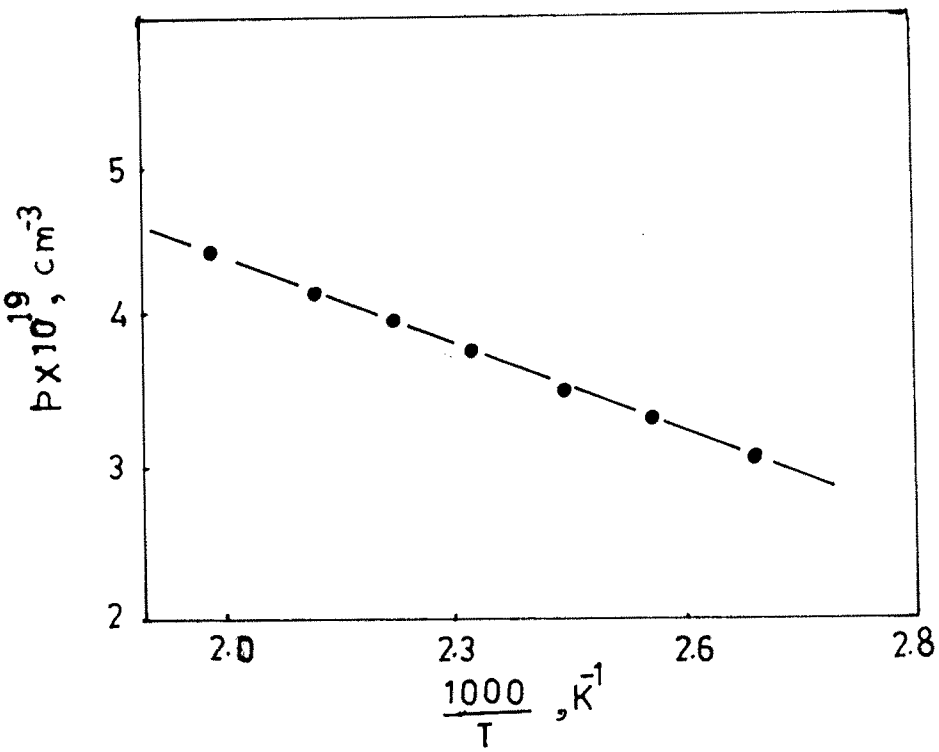

Fig. 3.10 Variation of the carrier concentration with reciprocal of the absolute temperature.

The grain barrier height (ϕ_B) was then determined from the log ($\mu T^{1/2}$) vs 1 / T variation and is shown in figure 3.11. The observed grin barrier height (ϕ_B) is 0.68 eV. It should be noted that the sum

$$E_{ap} + \phi_B = E_{a\sigma} \qquad \ldots(3.11)$$

which should be expected from the interrelationship of conductivity, carrier density and mobility. Here E_{ap} is the activation energy of the hole conduction, determined from the log p vs 1/T plot and is 0.0454 eV. In our case, it is seen that the relation (3.11) holds good.

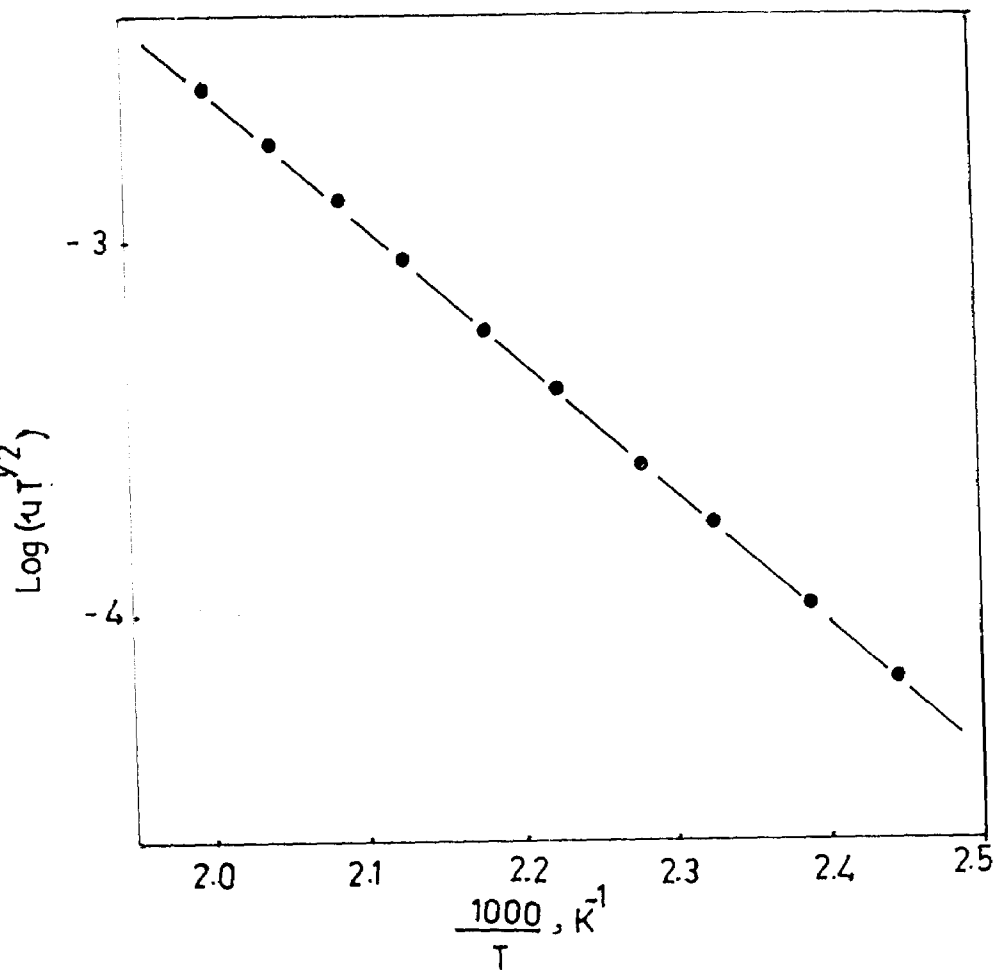

Fig. 3.11 Determination of intergrain barrier potential (ϕ_B) from the variation of log ($\mu T^{1/2}$) vs 1 / T for a typical SnS sample.

3.4 Conclusions

A chemical growth process is found to be one of the most suitable techniques to obtain the SnS thin film layers. The deposition is carried out in an alkaline medium and growth of the thin films is by slow release of Sn^{2+} and S^{2-} ions in a complex solution. Good quality deposition of SnS thin films with less consumption of both electrical power and active materials is made feasible. The as-deposited samples are brown chocolate in colour.

The structural and microscopic investigations of the sample revealed microcrystalline nature of the sample with orthorhombic crystal structure. The grain size determined using the Scherrer's relation is 267 A^{o}. The SEM observations showed well defined grains. Heat treatment improves crystalline nature. The data on optical studies showed a high absorption coefficient ($10^4 - 10^5$ cm $^{-1}$), direct mode of transitions and forbidden energy gap of 1.32 eV for as-deposited sample. SnS is highly resistive with a p-type conduction. The activation energies of an electrical conduction is 0.12 eV and 0.701 eV at low and high temperature regions, respectively. Thermally generated voltage is of the order of microvolts.

Table 3.1 Standard and observed X-ray diffraction data for a chemically grown SnS fim.

Peak No.	d (A^0)		hkl	I / I_{max}	
	obs.	JCPD		Obs.	JCPD.
1	4.073	4.04	011	31.6	16
2	3.27	3.24	102	55	40
3	2.81	2.83	013,004	100	100
4	2.33	2.30	104	56	32
5	2.03	2.02	114,022	28	24
6	1.67	1.69	123	26	16
7	1.55	1.56	025	45	3
8	1.41	1.40	032,008	35	13
9	1.27	1.26	118	28	10
JCPD - a = 3.99 A^o , b = 4.34 A^o, c = 11.20 A^o					

References

1. S. Chandra, in, "Photoelectrochemical Solar Cells, (ed) D. S. Compbell Gorden and Breech Science Publishers, N.Y , 1985.
2. Aruchami, G. Aravamudan and G. V. Subba Rao , Bull. Mater.Sci.4 (1982) 483.
3. B. T. Raut, D. S. Sutrave, V.B. Patil, G. S. Shahane and L. P. Deshmukh, National Seminar on Recent Trends in Materials Science, Sri Venkateshwara University, Tirupati, India, 25-28 Nov,1999.
4. B. T. Raut, V. B. Patil, E. U. Masumdar and L. P. Deshmukh, Proc. National Conference on Materials and Semiconductor Technologies in Electronic Research, G. B. Pant University of Agriculture and Technology, Pant Nagar (U. P.), India, 9-10 Nov., 2000.
5. B. T. Raut, V. B. Patil, P. D. More, V. S. Karande and L. P. Deshmukh, Ind. J. Pure & Appl. Phys. (Commun.)
6. J. E. Bauerie, P. H. Sutter and R. W. Ure Jr., in "Thermoelectricity: Science and Technology" (eds.) R. R. Heikel and R. W. Ure Jr., Interscience Publishers (1961) 285.
7. Joint Committee on Powder Diffraction Standards (JCPD) No. 1- 984 .
8. Hindenori Noguchi, A. Setiyadi, H. Tanamura, T. Nagatomo, O. Omoto., Solar Energy Mat. and Solar Cells 35 (1994) 325.
9. Sekhar C. Ray, Malay K. Karanjai, Dhruba DasGupta, Thin Solid Films 350 (1999) 72.
10. B. D. Cullity, in " Elements of X-ray Diffraction" , (2nd ed.) Addision – Wesly, INC. (1978) 102 .
11. D. S. Sutrave, G. S. Shahane, V. B. Patil and L. P. Deshmukh,

Turkish J. of Phys. 23 (1999) 1 .

12. D. Bhattacharya, S. Chaudhari and A. K. Pal, Vacuum 43 (1992) 313 .
13. G. S. Shahane, B. M. More, C. B. Rotti and L. P. Deshmukh, Mat. Chem. Phys. 47 (1997) 263 .
14. G. S. Shahane, Ph. D. Thesis, Shivaji University,Kolhapur, M. S.,India (1997).
15. Yu. I. Ravich, B. A. Efimova and Smirnov in "Methods of Semiconductor Investigations : Application to lead chalcogenides PbTe, PbSe and PbS " (I z d Nauka , Moscow) (1968) .
16. R. L. Petritz, Phys. Rev. 104 (1956) 1508.